



## Research article

# Salvianolic acid D: A potent molecule that protects against heart failure induced by hypertension via Ras signalling pathway and PI3K/Akt signalling pathway

Kai Chen<sup>a,b</sup>, Yiqing Guan<sup>a</sup>, Shaoyu Wu<sup>c</sup>, Dongling Quan<sup>c</sup>, Danni Yang<sup>c</sup>,  
Huanxian Wu<sup>c</sup>, Lin LV<sup>c,\*\*</sup>, Guohua Zhang<sup>a,\*</sup>

<sup>a</sup> School of Traditional Chinese Medicine, Southern Medical University, China

<sup>b</sup> Shenzhen Hospital, Southern Medical University, China

<sup>c</sup> School of Pharmaceutical Sciences, Southern Medical University, China



## ARTICLE INFO

## Keywords:

Salvianolic acid D  
Heart failure  
Hypertension  
Cardiomyocyte  
Mitochondrial

## ABSTRACT

**Ethnopharmacological relevance:** Salvianolic acid D (Sal D) is a natural substance extracted from *Radix Salviae* that performs a cardiovascular benefit. However, the protective mechanism of Sal-D for heart failure remains uncertain.

**Aim of the study:** In this study, we aim to evaluate the effect of Sal D on heart failure and elucidate its underlying mechanisms.

**Materials and methods:** Using the spontaneously hypertensive rats (SHR) as a cardiac remodelling model, the cardioprotective effect of Sal D was evaluated. Employing bioinformatics analysis, the related mechanisms of Sal D treatment on heart failure were identified and validated by Western blot and polymerase chain reaction.

**Results:** The results showed that Sal D significantly improved cardiac function and attenuated cardiac hypertrophy. Besides, Sal D impaired mitochondrial structure and restored the energy charge of cardiomyocytes managed by angiotensin II. Bioinformatics analysis suggested that Sal D might improve heart failure by modulating the Ras and PI3K/AKT signalling pathways verified in vitro and in vivo.

**Conclusion:** In summary, Sal D can improve the heart function of SHR by inhibiting the Ras signalling pathway and activating the PI3K/AKT signalling pathway.

## 1. Introduction

According to an epidemiological survey around the world, one in five people suffer from heart failure at some stage of their lives, usually in the elderly [1]. Therefore, when a country enters an ageing society, the population with heart failure will grow increasingly. Even in advanced medical developed countries, heart failure cannot be cured entirely. Conventional treatments for HF include diuretics, angiotensin receptor blockers, angiotensin-converting enzyme inhibitors, beta-blockers, and aldosterone receptor antagonists [2]. While medical treatment has reduced the morbidity and mortality of HF, additional treatment is needed to improve clinical

\* Corresponding author.

\*\* Corresponding author.

E-mail addresses: [lynnlv@smu.edu.cn](mailto:lynnlv@smu.edu.cn) (L. LV), [zghgz@163.com](mailto:zghgz@163.com) (G. Zhang).

outcomes because of the high mortality rate.

Compared with western medicine, the abundant treasury of traditional Chinese medicine (TCM), with a history of thousands of years, has unique theories and technology. It is an indispensable part of the medical and health system with Chinese characteristics. As a gift from traditional Chinese medicine to the world, artemisinin is Tu Youyou's inspiration in reviewing Gehong's "ZhouhouBeiji Fang," an ancient medical book written more than 2000 years ago [3]. Therefore, screening safe and effective medicine from TCM is not only for pharmacological development but also has clinical utility.

DanShen, the root of a natural herbal *Salvia miltiorrhiza Bunge.*, is commonly used in the treatment of HF patients [4]. The extracted phenolic acid monomer Salvianolic acid D (SalD) is one of the significant antioxidants from Danshen with increasing research interest. Recent studies have shown that SalD showed potential antiplatelet activity and peroxidase inhibition [5]. Moreover, SalD has been identified as a valuable compound found in the Danhong injection used to relieve vascular endothelium impairment used for the treatment of acute myocardial infarction [6]. Compared with the famous ingredients in DanShen, just like tanshinone I, tanshinone IIA, and Salvianolic acid A, which have a considerable improvement in heart failure [7–9], the research on biological effects of Sal D is restricted.

In this experiment, we tried to explore the specific mechanism of Sal D on heart failure. The spontaneously hypertensive rats (SHR) were used as an animal model to evaluate the effects of Sal D in the treatment of HF. Bioinformatics technology is applied to reveal the action mechanism.

## 2. Materials and methods

### 2.1. Reagents and drugs

Salvianolic acid D (CAS: 142998-47-8, purity  $\geq 98\%$ ) was purchased from Wuhan ChemFaces Biochemical Co., Ltd. (Wuhan, China). Losartan Tablets (12.5 mg, Lot H20000371) as the positive control were provided by Bristol-Myers Squibb Co., Ltd. (Shanghai, China). Honokiol (CAS: 35354-74-6) was purchased from MedChem Expression Co., Ltd. (Beijing, China).

### 2.2. Animal grouping and administration

Animal treatment protocols were based on institutional Animal ethical committee guidelines, which in light of the Guide for the Care and Use of Laboratory Animals published by the United States National Institutes of Health (NIH Publications No. 85-23, revised 1996) and with the approval of the Animal Care Committee of Southern Medical University (Approval No. L2021080).

The experiment was performed on 40 male spontaneously hypertensive rats (SHR) at 16 weeks old and eight sex- and age-matched Wistar-Kyoto (WKY) rats, which were purchased from Vital River Laboratory Animal Technology Co., Ltd., (Beijing, China; certificate number: SCXK2019-0025) and kept in the SPF level conditions at Southern Medical University under controlled temperature at 22–24 °C, humidity at 40  $\pm$  5% and a 12 light/dark cycle. All rats were allowed free access to water and food.

After one week's acclimation, the rats were randomly divided into six groups (number/group = 8): WKY group (Normal control), SHR group (cardiac remodelling model), LOS group (SHR + losartan, 13.5 mg kg<sup>-1</sup>·d<sup>-1</sup>), SDL group (SHR + Sal D low dose, 1 mg kg<sup>-1</sup>·d<sup>-1</sup>), SDM group (SHR + Sal D medium dose, 3 mg kg<sup>-1</sup>·d<sup>-1</sup>), SDH group (SHR + Sal D high dose, 10 mg kg<sup>-1</sup>·d<sup>-1</sup>). SDL, SDM, SDH, and LOS groups were orally administered every day for 12 weeks with their corresponding group assignment, whereas WKY and SHR groups received the same volume of distilled water. Sal D was dissolved with 1% DMSO (dimethyl sulfoxide).

### 2.3. Blood pressure and echocardiography measurements

After 12 weeks of administration, systolic blood pressure (SBP) and diastolic blood pressure (DBP) were determined using the tail-cuff method (ALC-NIBP, Shanghai Alcott Biotechnology Co., Ltd., Shanghai, China). Briefly, rats were preheated at 30 °C for 10 min, and five stable consecutive measurements of blood pressure were averaged. Besides, heart rate (HR), ejection fraction (EF), and fractional shortening (FS) were detected by the Color Doppler ultrasound in M-Mode and its corresponding probe in a 10-MHz frequency (S40 Exp, Shenzhen City Science and Technology Co., Ltd., Shenzhen, China).

### 2.4. Histopathological detection

After rats were executed with narcotic overdose, the heart was separated quickly and weighed for the HW/BW index (heart weight to body weight ratio). The heart was cut horizontally at the maximum diameter, and the left ventricle tissues were dissociated and fixed with 4% paraformaldehyde for 24 h. Specimens were paraffin-embedded, sliced at 5 mm, and stained with Masson's Trichrome (Solarbio, USA) for fibrillar collagen. Collagen degree was quantified in 10 random visual fields per section as collagen volume fraction (CVF) with a light microscope (CX31, Olympus, Tokyo, Japan) at 40  $\times$  magnification ImageJ software (National Institutes of Health, Bethesda, MD, USA). For measuring the cardiac myocyte cross-sectional areas, paraffin-embedded sections were dewaxed and rehydrated in graded ethanol. The sections were stained with wheat germ agglutinin lectin (WGA) (FITC) (0.1 mg/mL) (GeneTex, Irvine, CA, USA), and the nuclei were counterstained with DAPI. The degree of apoptosis in heart tissue was further observed by staining using the terminal deoxynucleotidyltransferase-mediated dUTP nick end labelling (TUNEL) reagent kit according to the manufacturer protocol (Beijing Solarbio Technology Co., Ltd, China).

## 2.5. Electron microscopy

The anterior walls of the left ventricle were fixed in 2.5% glutaraldehyde and 1% paraformaldehyde at four °C for 24 h and then washed with 0.1 M phosphate-buffered solution at 4 °C, stained in 2% osmium tetroxide, embedded and sectioned. After washing twice, the tissues were postfixed with a 1% OsO<sub>4</sub>-buffered solution (pH 7.4) for 1 h. After being dehydrated and embedded, the resins were sectioned using an EM Ultramicrotome LKB-2088 and stained with 1% toluidine blue. The ultrathin sections were then double-stained with uranyl acetate and lead citrate and examined with a Hitachi H-7500 electron microscope (Hitachi, Tokyo, Japan).

## 2.6. Adenine nucleotide analysis

Heart tissues and cardiomyocytes were transferred to ice-cold 0.6 M HClO<sub>4</sub> (4 mL/g) and immediately homogenized and centrifuged at 10 000 g for 10 min at 4 °C. The supernatant was neutralized and filtered after centrifuging under the same conditions. Next, samples were determined via a high-performance liquid chromatography (HPLC) method with a Waters C18 column (250 × 4.6 mm, five μm). Analytes were isocratic ally eluted using 96% 0.05 M KH<sub>2</sub>PO<sub>4</sub> (pH 6.5) and 4% methanol for 20 min. Concentrations of adenosine triphosphate (ATP), adenosine diphosphate (ADP), and adenosine monophosphate (AMP) were measured at 254 nm through a standard external method for quantification. The energy charge was calculated as (ATP + ADP/2)/(ATP + ADP + AMP).

## 2.7. Culture of primary cardiomyocytes

Primary cultures of neonatal rat cardiomyocytes were conducted as in the previous study [6]. Briefly, neonatal SD rats were sacrificed, and the hearts were quickly excised and minced through fine microbic scissors, then further digested via D-Hanks' solution containing 0.1% trypsin at 37 °C for 5 min. Cells were isolated by 5-min rounds of tissue digestion 8 to 10 times. After incubation, the supernatant was added to an equal volume of Dulbecco-modified Eagle media containing 10% fetal bovine serum (FBS). The total cell supernatants were centrifuged at 1000 rpm for 10 min. Supernatants were discarded, and the cell pellets were resuspended in media containing 10% FBS. The cells were plated onto 100-mm culture dishes at  $1 \times 10^5$  cells per square centimetre. The cardiomyocytes were cultured in an incubator filled with a humidified atmosphere of 5% CO<sub>2</sub> at 37 °C.

For investigating the cardioprotection of Sal D, cells were divided into six groups: (1) control (CON) group: cells were incubated with high-glucose DMEM containing 10% FBS without angiotensin II and Sal D for 48 h in all; (2) angiotensin II (ANG) group: cells were incubated with 1 μM angiotensin II for 24 h in DMEM as previously described without Sal D treatment; (3) ANG + low dose Sal D (SDL) group: cells were pretreated with 1 μM Sal D for 24 h before induction of ANG; (4) ANG + medium-dose Sal D (SDM) group: cells were pretreated with 3 μM Sal D for 24 h before induction of ANG; (5) ANG + high-dose Sal D (SDM) group: cells were pretreated with 10 μM Sal D for 24 h before induction of ANG; (6) ANG + losartan (LOS) group: cells were infected with 1 μM losartan for 24 h before installation of ANG.

For investigating the molecular mechanism of Sal D, cells were divided into eight groups: (1) cells were incubated with high-glucose DMEM containing 10% FBS without ANG, Sal D, and Honokiol for 48 h in all; (2) cells were incubated with 1 μM ANG for 24 h in DMEM as previously described without Sal D and honokiol treatment; (3) cells were treated with 10 μM Sal D for 24 h without incubation of ANG and Honokiol; (4) cells were pretreated with 1 μM Honokiol for 24 h without incubation of ANG, and Sal D; (5) cells were treated with 10 μM Sal D, and 1 μM Honokiol for 24 h without induction of ANG; (6) cells were pretreated with 1 μM Honokiol for 24 h before incubation of ANG without treatment of Sal D; (7) cells were pretreated with 10 μM Sal D for 24 h before induction of ANG without incubation of Honokiol, and (8) cells were pretreated with 10 μM Sal D and 1 μM Honokiol for 24 h before induction of ANG for 24 h. Honokiol (CAS # 35354-74-6) is a biphenyl neolignan and active part of Magnolia extract that inhibits phosphorylation of Akt, p44/42 mitogen-activated protein kinase (MAPK), and activates phosphorylation of Ras.

## 2.8. Molecular mechanism analysis

A similarity-based method is implemented in the bioinformatics analysis tool for the molecular mechanism of the traditional medicine platform (BATMAN-TCM, <http://bionet.ncpsb.org/batman-tcm>) and the traditional Chinese medicine systems pharmacology database and analysis platform (TCMSP, <http://lsp.nwu.edu.cn/index.php>) were used to predict potential targets of Sal D, which further screened out using Pharmmapper Server (<http://lilab.ecust.edu.cn/pharmmapper>). After obtaining from the database, we performed KEGG analysis through a plug-in ClueGO in Cytoscape 3.7.1 (<https://cytoscape.org/>) to clarify the signalling pathways related to Sal D on cardiac remodelling ( $P < 0.05$ , Min Overlap  $\geq 3$ ).

## 2.9. Real-time PCR

Myocardial tissue was homogenized in TRIzol Reagent (Ambion, 15596026, USA) to extract RNA. Double-stranded cDNA was synthesized from 5 μg of total RNA with Revert Aid First Strand cDNA Synthesis Kit (Thermo Fisher Scientific, K1622, USA). The real-time PCR analysis was conducted via SYBR Select Master MIX (Applied Biosystems, 4472908, USA) and the sequences of the following primers.  $2^{-\Delta\Delta Ct}$  method was applied to obtain relative gene expression.

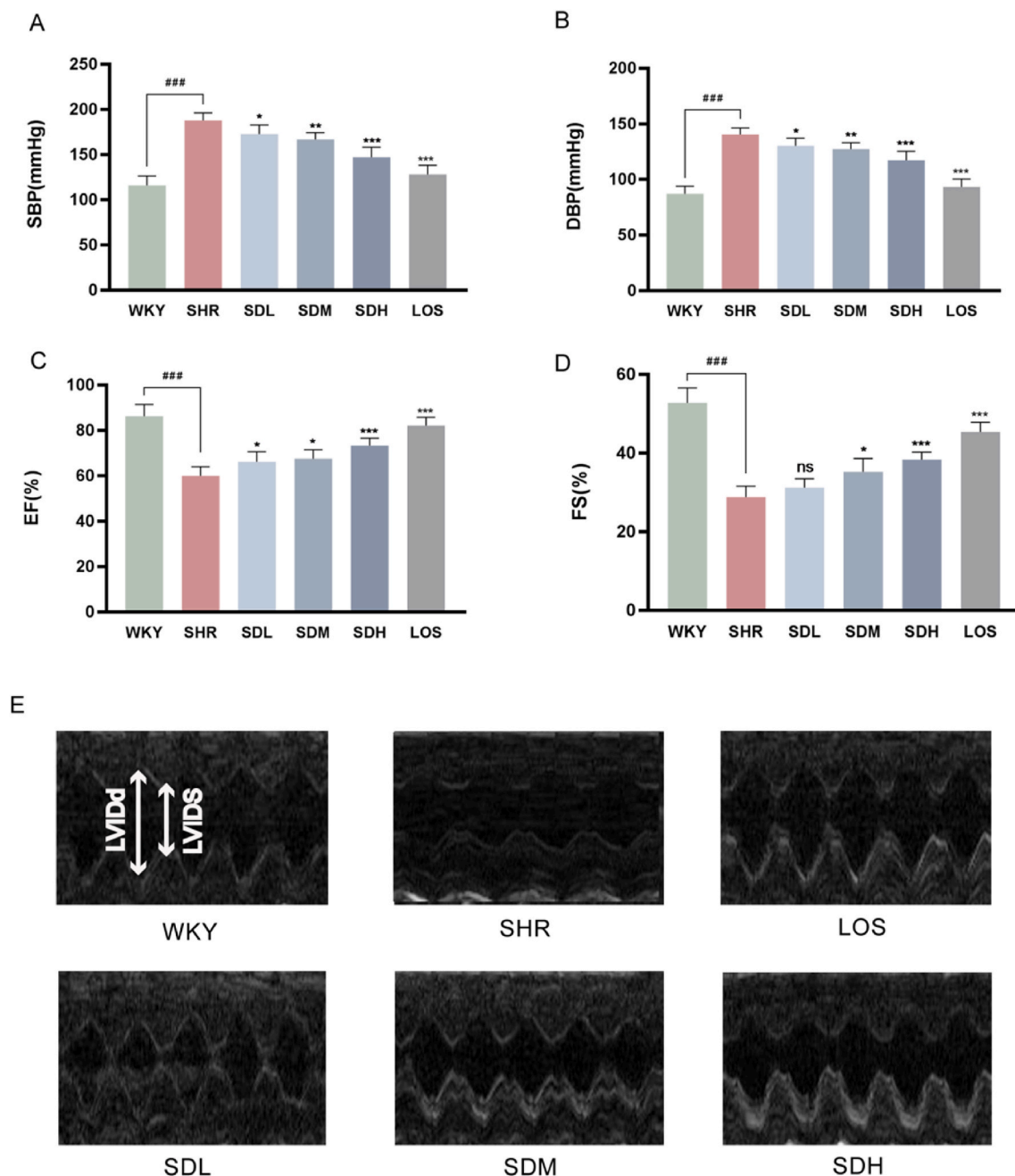


**Fig. 1.** The effects of Sal D treatment on blood pressure and cardiac function after administration for 12 weeks. (A) SBP; (B) DBP; (C) EF; (D) FS; (E) Represented image of ultrasound cardiogram.  $n = 8$ . ###,  $P < 0.001$  vs. WKY. ##,  $P < 0.01$  vs. WKY. #,  $P < 0.05$  vs. WKY. \*\*\*,  $P < 0.001$  vs. SHR. \*\*,  $P < 0.01$  vs. SHR. \*,  $P < 0.05$  vs. SHR.

## 2.10. Western blotting

The total proteins were extracted from the myocardium and cardiomyocytes. The protein concentrations were detected using the BCA protein assay reagent (Thermo, 23225). Protein samples (20  $\mu\text{g}$ ) in a gel were separated on 10% SDS/PAGE and then transferred into a polyvinylidene fluoride (PVDF) membrane (Millipore, Beijing, China) via a Gel Transfer Device (Invitrogen). After PVDF, the

**Table 1**  
Changes in heart rate, body weight, heart weight, relative heart weight, LVIDd, and LVIDs in rats.

Groups	Heart rate (per minute)	Body weight (g)	Heart weight (g)	Relative heart weight	LVIDd (mm)	LVIDs (mm)
WKY (normal control))	361.6 ± 6.43	272.9 ± 8.86	0.84 ± 0.06	3.09 ± 0.25	6.28 ± 0.17	2.43 ± 0.41
SHR (positive control)	475 ± 14.05 <sup>###</sup>	266.02 ± 7.65	1.32 ± 0.06 <sup>###</sup>	4.95 ± 0.3 <sup>###</sup>	8.83 ± 0.67 <sup>###</sup>	5.67 ± 0.46 <sup>###</sup>
SDL (SHR + Sal D low dose)	425.2 ± 18.43 <sup>**</sup>	267.82 ± 11.56	1.25 ± 0.08	4.67 ± 0.19	7.93 ± 0.24 <sup>***</sup>	4.57 ± 0.29 <sup>**</sup>
SDM (SHR + Sal D medium dose)	400.8 ± 11.86 <sup>***</sup>	271.52 ± 10.31	1.12 ± 0.04 <sup>***</sup>	4.12 ± 0.23 <sup>**</sup>	7.18 ± 0.34 <sup>***</sup>	4.29 ± 0.21 <sup>***</sup>
SDH (SHR + Sal D high dose)	386.4 ± 7.3 <sup>***</sup>	265.68 ± 6.06	1.06 ± 0.08 <sup>***</sup>	3.98 ± 0.26 <sup>***</sup>	6.73 ± 0.27 <sup>***</sup>	3.77 ± 0.35 <sup>***</sup>
LOS (SHR + losartan)	365.8 ± 8.87 <sup>***</sup>	266.74 ± 7.8	0.97 ± 0.09 <sup>***</sup>	3.64 ± 0.3 <sup>***</sup>	6.52 ± 0.19 <sup>***</sup>	3.51 ± 0.23 <sup>***</sup>

<sup>###</sup>,  $P < 0.001$  vs. WKY. <sup>##</sup>,  $P < 0.01$  vs. WKY. <sup>#</sup>,  $P < 0.05$  vs. WKY. <sup>\*\*\*</sup>,  $P < 0.001$  vs. SHR. <sup>\*\*</sup>,  $P < 0.01$  vs. SHR. <sup>\*</sup>,  $P < 0.05$  vs. SHR.

membranes were incubated with primary antibodies against p-Ras, Ras, p-Raf(ser338), Raf, p-Mek (ser217), Mek, p-Erk(Thr202), Erk, p-PI3K, PI3K, p-AKT (Thr308), AKT, and Gapdh for over-night at 4 °C. After washing with PBST, the membranes were probed with secondary antibodies conjugated to horseradish peroxidase (HRP) at room temperature. The quantification of Western blotting bands was performed with the Odyssey infrared imaging system (Li-Cor Biosciences). Corresponding protein expression levels were normalized to the GAPDH protein level.

### 2.11. Statistical analysis

Data are presented as mean ± SEM. Multiple group comparisons were carried out using one-way analysis of variance (ANOVA) followed by Tukey–Kramer or Dunnett test for posthoc analysis. Statistical significance was acceptable to a level of  $P < 0.05$ . Data analysis was achieved using SPSS 16.0.

## 3. Results

### 3.1. The effect of Sal D on blood pressure, heart rate, and cardiac function

Changes in systolic blood pressure (SBP) and diastolic blood pressure (DBP) for rats are shown in Fig. 1A and B. After administration for 12 weeks, both SBP and DBP of the SHR group were evidently higher than those in the WKY group (Fig. 1A and B). With the administration of Sal D, blood pressure was decreased in a dose-dependent manner, but the overall effects were not as credible as in the LOS group.

Heart rate (HR), ejection fraction (EF), and fractional shortening (FS) were used to evaluate the cardiac function of rats, while the impairment of EF and FS suggested cardiac functional insufficiency. As exhibited in Table 1, the HR in the SHR group was higher than that in the WKY group, while the HR changes were significantly attenuated by Sal D and LOS. Moreover, Sal D and LOS treatments increased EF and FS compared with those in the SHR group (Fig. 1C and D). Representative images of ultrasound cardiograms in M-mode are shown in Fig. 1E.

### 3.2. The effects of Sal D treatment on cardiac hypertrophy and myocardial injury

Consistent with the increase in blood pressure and reduction of cardiac function, significant deterioration of myocardial hypertrophy via histological analysis was shown in SHR compared with WKY, as evidenced by the increase in the ratio of HW/BW (relative heart weight). Lvids and LVIDd were also significantly increased in SHR compared with WKY ( $P < 0.001$ ) in Table 1. The treatment of Sal D prevented cardiac hypertrophy and decreased HW/BW, LVIDs and LVIDd compared with SHR.

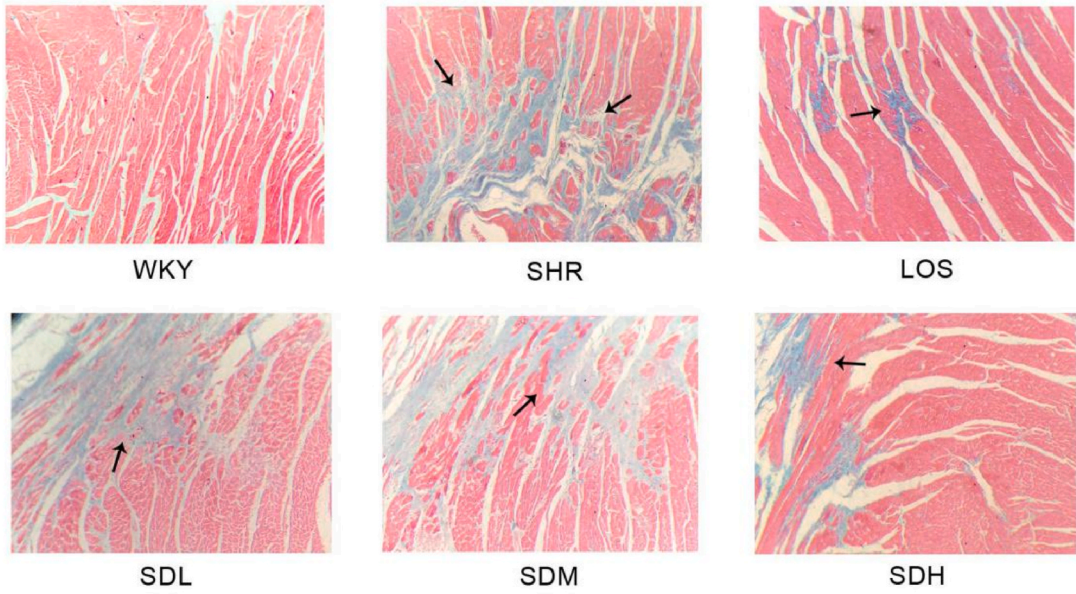
Using Masson's trichrome staining (Fig. 2A), we found that the content of cardiac collagen (stained in blue colour) under Sal D treatment was significantly decreased in a dose-dependent manner compared with SHR (40 × magnification), which was further supported by the alleviation of CVF (Fig. 3B). Moreover, we investigated the effect of Sal D on the mRNA levels of A-type natriuretic peptide (ANP) and brain natriuretic peptide (BNP), two crucial cardiac hypertrophic markers. Compared with the WKY group, SHR significantly increases the expression of ANP ( $P < 0.05$ ) and BNP ( $P < 0.001$ ) mRNA expression. In contrast, Sal D not only down-regulated the expression level of ANP mRNA but significantly inhibited the expression level of BNP mRNA ( $P < 0.001$ ) (Fig. 2C and D).

The protective effect of Sal D on cardiac hypertrophy and apoptosis was further determined using WGA staining and TUNEL assay, respectively. In comparison with the WKY group, SHR significantly increased the cell size of cardiomyocytes ( $P < 0.001$ ), which was primarily abrogated by Sal D (Fig. 3A and C). Furthermore, as shown by the tagged nuclei in red fluorescence, an indicator of apoptosis, the SHR group markedly increased in myocardial tissue compared with the WKY group ( $P < 0.001$ ) (Fig. 2B and D). However, Sal D inhibited this increase in cardiomyocyte apoptosis compared with the control group.

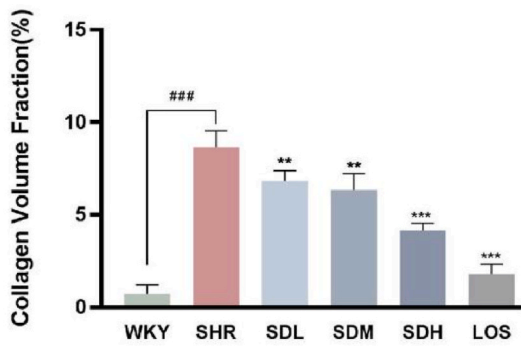
### 3.3. The effect of Sal D on mitochondrial morphology and mitochondrial function in the myocardium

Ultrastructural analysis of the myocardium showed apparent morphological changes in the SHR group compared with those in the WKY group (Fig. 4A). The electron microscopic observation on mitochondria demonstrated that the mitochondrial density was lower

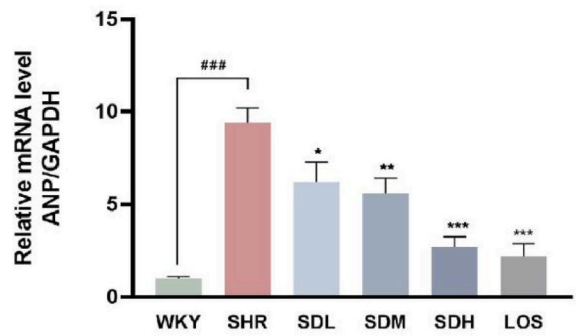
A



B



C



D

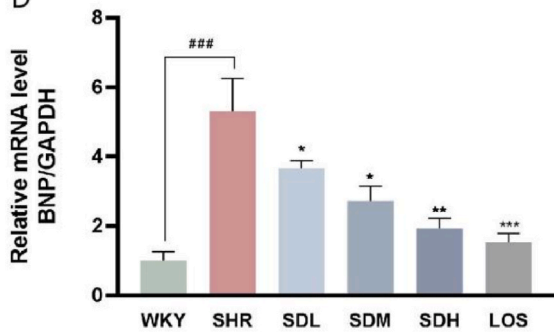


**Fig. 2.** The effects of Sal D treatment on myocardial injury. (A) Masson staining images under 200 × magnification and the areas of collagen deposition were indicated by the black arrow; (B) CVF; (C–D) Quantification of expression levels of ANP and BNP mRNA in heart tissue were measured using Real-time PCR (n=3).  $2^{-\Delta\Delta Ct}$  method was used to analyze relative gene expression levels. (\* $P < 0.05$ , \*\* $P < 0.01$  and \*\*\* $P < 0.001$  vs. SHR; ### $P < 0.001$  vs. WKY).

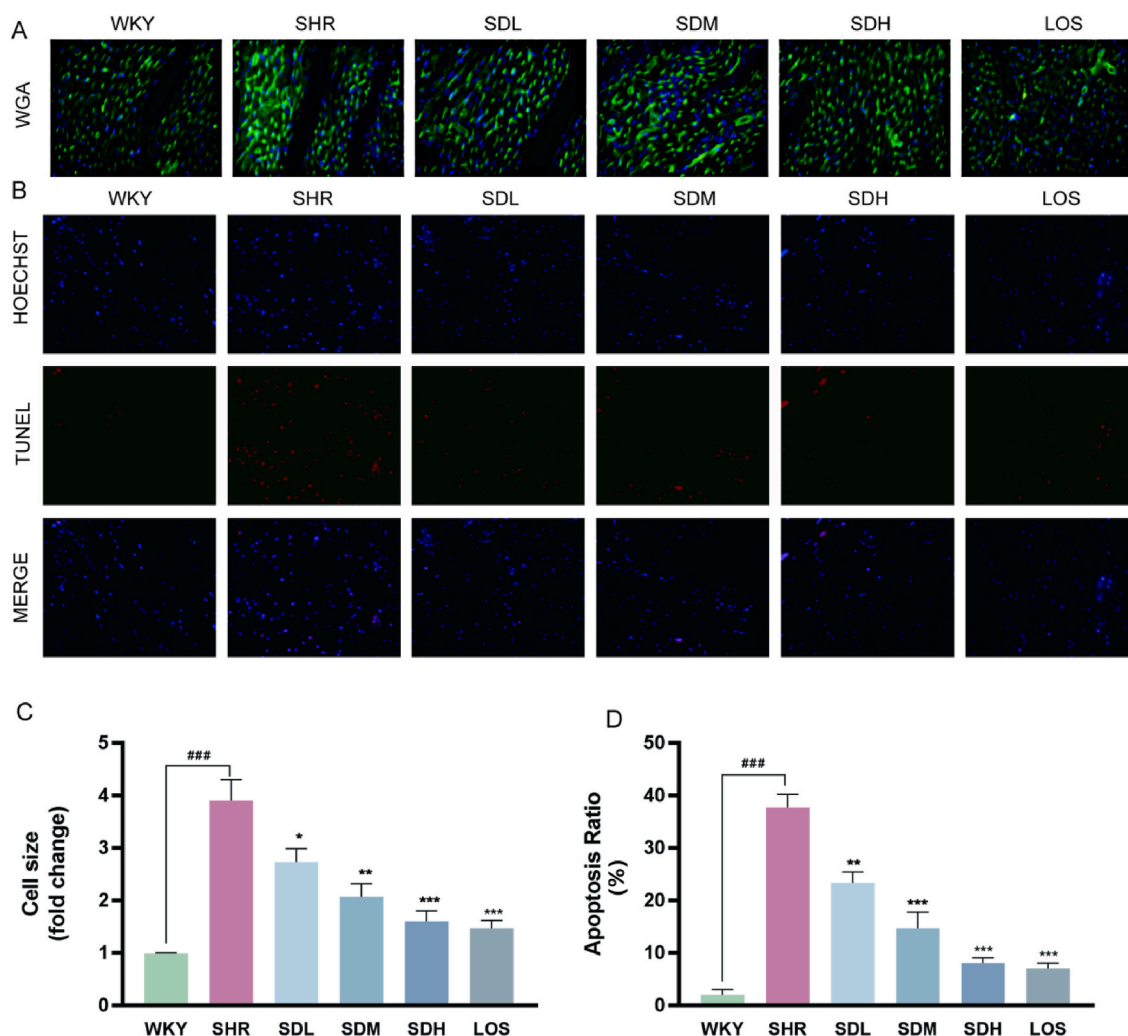


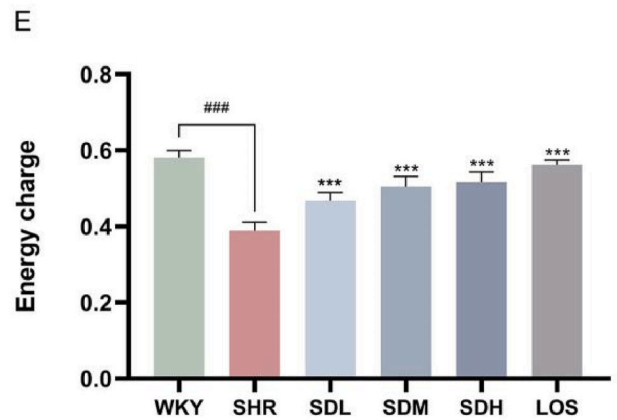
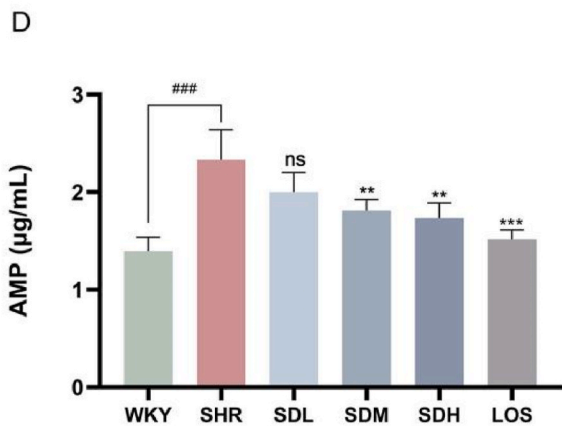
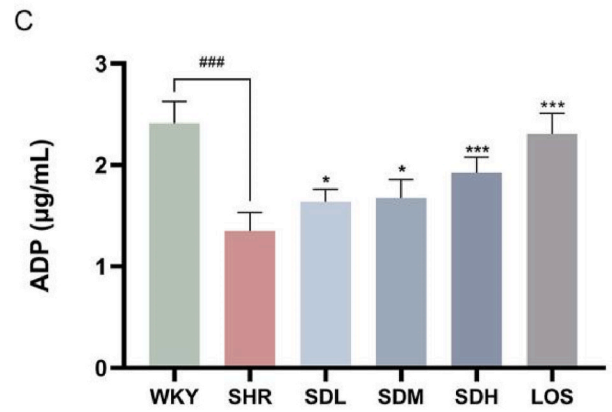
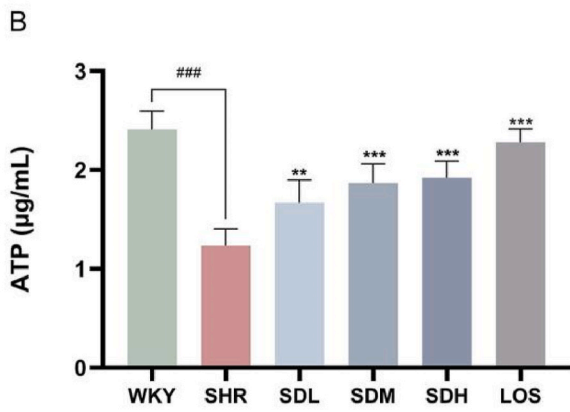
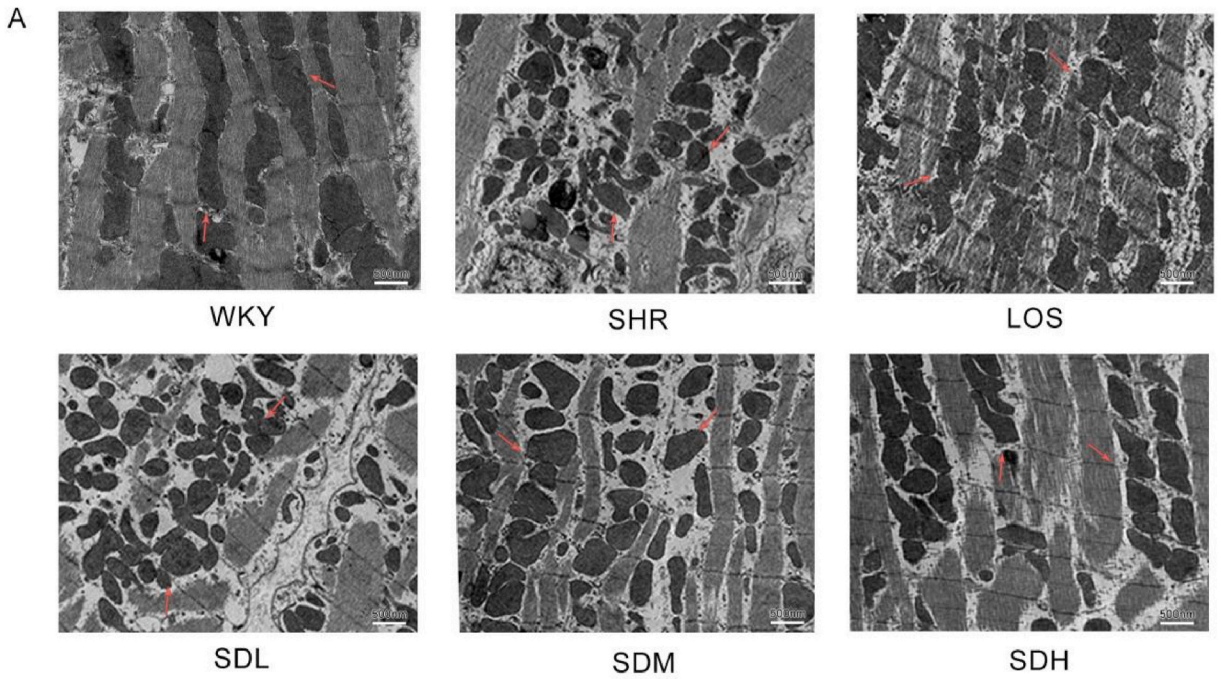
**Fig. 3.** The effect of Sal D on myocardial hypertrophy and apoptosis. (A) WGA was performed to determine cardiomyocytes' cross-sectional area (magnification  $\times 400$ ) ( $n = 5$ ). (B) The degree of apoptosis in heart tissue was analyzed using TUNEL staining. The nucleus was blue by staining with HOECHST, and positive apoptosis cardiomyocytes were red by staining with TUNEL reagent (magnification  $\times 400$ ) ( $n = 5$ ). Scale bars 100  $\mu\text{M}$ . (C) Quantification of the fold change of cardiomyocyte size was displayed. (D) Quantification of the percentage of apoptotic cells was exhibited. ###,  $P < 0.001$  vs. WKY. ##,  $P < 0.01$  vs. WKY. #,  $P < 0.05$  vs. WKY. \*\*\*,  $P < 0.001$  vs. SHR. \*\*,  $P < 0.01$  vs. SHR. \*,  $P < 0.05$  vs. SHR. (For interpretation of the references to colour in this figure legend, the reader is referred to the Web version of this article.)

in the myocardium of the SHR group and showed a more significant variation in dimension. The myocardium structure from the SHR group exhibited fuzzy striation, fewer cristae structures, and even complete disappearance of the z line. Conversely, the Sal D treatment restored the damage to mitochondrial morphology and the construction of mitochondria.

The mitochondrial function characterized as energy production was evaluated via the quantification of adenine nucleotide variants in the myocardium. The results showed that the Sal D treatment promoted the concentrations of ATP and ADP in the myocardium, while those in the SHR group were lower than in the WKY group (Fig. 4B–D). Conversely, AMP concentration was higher in the SHR group compared with the WKY group, while the Sal D treatment reduced it. Overall, the Sal D groups, especially in high doses, have a higher energy charge than the SHR group (Fig. 4E).

### 3.4. Exploration of the molecular mechanisms of Sal D

Through the TCMS database and BATMAN-TCM, we obtained 9 potential molecular targets of Sal D (Table 2). Then, PharmMapper Server was retrieved, and finally, 21 molecular targets were screened out as molecular targets of Sal D (Table 3). Signalling pathways that enriched via the molecular targets were shown in Fig. 5A and B and Table 4. As a result, the Ras signalling pathway and



(caption on next page)



**Fig. 4. Changes in mitochondrial morphology and mitochondrial function.** (A) Ultrastructural analysis of myocardium under 25000 × magnification and the areas of mitochondrion were marked by the red arrow. (B–E) ATP, ADP, AMP concentrations, and energy charge in the myocardium. ###,  $P < 0.001$  vs. WKY. ##,  $P < 0.01$  vs. WKY. #,  $P < 0.05$  vs. WKY. \*\*\*,  $P < 0.001$  vs. SHR. \*\*,  $P < 0.01$  vs. SHR. \*,  $P < 0.05$  vs. SHR. (For interpretation of the references to colour in this figure legend, the reader is referred to the Web version of this article.)

**Table 2**

Target data of Sal D from the TCMSP and BATMAN-TCM.

TCMSP	BATMAN-TCM
F2, F10, Ptgs2, Prss1	Pik3cb, Mapk1, Pck2, Ptgs2, Ptk2, Jnk

**Table 3**

Target data of Sal D from Pharmmapper Server.

Pharmmapper Server
Pik3ca, Rras2, Rap1b, RIP1, Akt1, Mapk3, Pik3cb, Pik3cd, Cdk3, Hras, Raf1, Mras, Mtor

PI3K-AKT signalling pathway may be the potential signalling pathway that Sal D treats for heart failure.

### 3.5. The effect of Sal D on the Ras signalling pathway and PI3K/AKT signalling pathway

Mitochondrial redox signalling pathways are mainly mediated by Ras, Raf, Mek, and Erk. Western blot analysis revealed that the protein expression levels of p-Ras, p-Raf, p-Mek, and p-Erk were increased in the SHR group compared with that in the WKY group to different degrees, while treatment with Sal D decreased the levels in a dose-dependent manner (Fig. 6A–I). A similar result was observed in cardiomyocytes (Fig. 7A–I).

### 3.6. Mechanism of Sal D on Ras and PI3K/AKT signalling pathway

To clarify the mechanism of Sal D on Ras and PI3K/AKT signalling pathway in cardiomyocytes, the cardiomyocytes were exposed to Sal D, Ang II, and Honokiol, or the combination at indicated concentrations. Besides, a Western blot was conducted. The results revealed that Ang II and Honokiol enhanced the protein expression of p-Ras, p-Raf, p-ERK, and p-MEK and inhibited the protein expression of p-Pi3k, p-Akt (Fig. 8A–I). Significantly, the repression of the Ras signalling pathway and enhancement of the PI3K/AKT signalling pathway on Sal D was reversed by Honokiol.

## 4. Discussion

This research aims to explain the effect and mechanism of Sal D on HF. The typical pathological changes of HF, containing the thickened left ventricle, reduced heart function, growing collagen, hypertrophic cardiomyocyte, and aggravated myocardial apoptosis in the myocardium, were observed in the SHR consistent with the previous reports [10]; Pluteanu e Nikonova et al., 2018). The ejection fraction (EF) and fractional shortening (FS) were detected as an indicator of cardiac function. Like ANP, BNP is a primary endocrine system for the human body to resist capacity overload and hypertension [11]. The pharmacological experiment suggested that Sal-D improved LVIDs significantly in SHR, followed by increasing EF and FS. Under the treatment of Sal-D, the arrangements of myocardial cells were much more neatly and tightly.

Furthermore, minor collagen tissues were observed in myocardiocytes. The deposition of collagen and cardiomyocyte hypertrophy and apoptosis were improved under the Sal-D treatment, as well as the collagen volume fraction in the myocardium. Furthermore, Sal-D can improve the mRNA overexpression of ANP and BNP, which showed benefit to the protection of ventricular function and the improvement of pathological reconstruction. Summarized the information given above, administrated with Sal D altered cardiac injury index of function in SHR, repaired injured myocardium, and ameliorated heart function.

As another vital indicator for assessing HF, the function of mitochondria was designed in this study to investigate the oxygen uptake rate of cardiomyocytes. On account of mitochondria, density occupying 40%–60% of the total volume of cardiomyocytes to give the highest oxygen uptake rate of the heart in the body [12], the dysfunction of mitochondria will lead to an attenuation of myocardial energy metabolism, which have crucial impact on the progression of heart failure [13]. Previous studies reported that hypertension is a severe factor that induces mitochondrial dysfunction in the myocardium [14], which presents mitochondrial structure damage and decreased the permeability of mitochondrial membrane potential in cardiomyocytes.

Bioinformatics technology was employed in this study to explore the specific mechanism of Sal D on HF, including TCMSP, a unique systems pharmacology platform of Chinese herbal medicines that captures the relationships between drugs, targets, and diseases [15]. BATMAN-TCM, the first online bioinformatics analysis tool specially designed for the research of the molecular mechanism of TCM, is mainly based on TCM ingredients' target prediction and the following network pharmacology analyses of the potential targets [16]. Pharmmapper Server is a silicon target prediction method of developing for a given small molecule by probing the potential ligand-binding sites via ligand-protein reverse docking strategy [17]. With appliance with these databases and functional enrichment

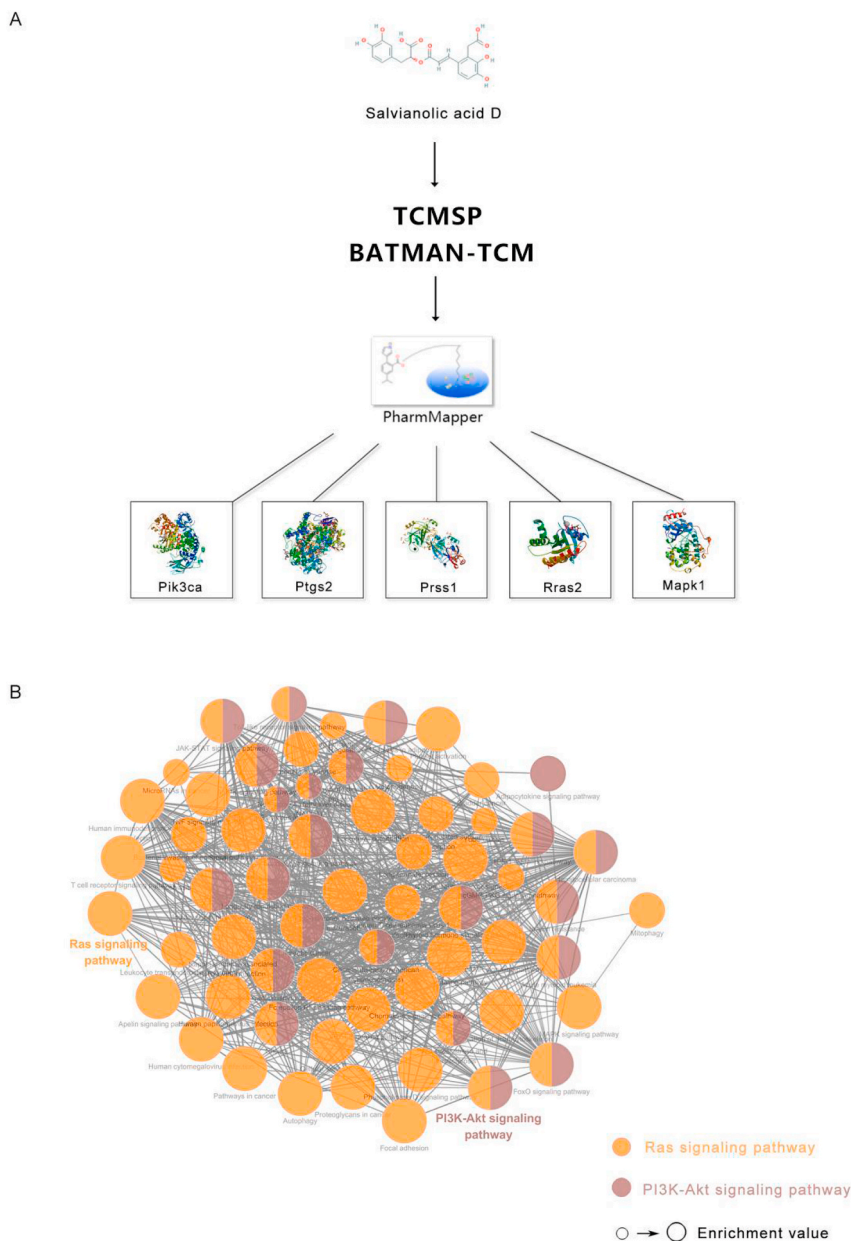


**Fig. 5. Functional enrichment analysis of signalling pathways of Sal D treating heart failure.** (A) Flow chart of targets searched via TCMSP, BATMAN, and PharmMapper. (B) Significantly enrichment of protein targets in the network diagram.

**Table 4**  
Functional enrichment analysis of protein targets related to Sal D.

Function	Count	FDR
Ras signalling pathway	9	0.001372
PI3K-AKT signalling pathway	9	0.031572
JAK-STAT signalling pathway	6	0.018323
HIF-1 signalling pathway	5	0.001928
TNF signalling pathway	5	0.027431
Toll-like receptor signalling pathway	4	0.008342
VEGF signalling pathway	4	0.009012
Apelin signalling pathway	4	0.028155

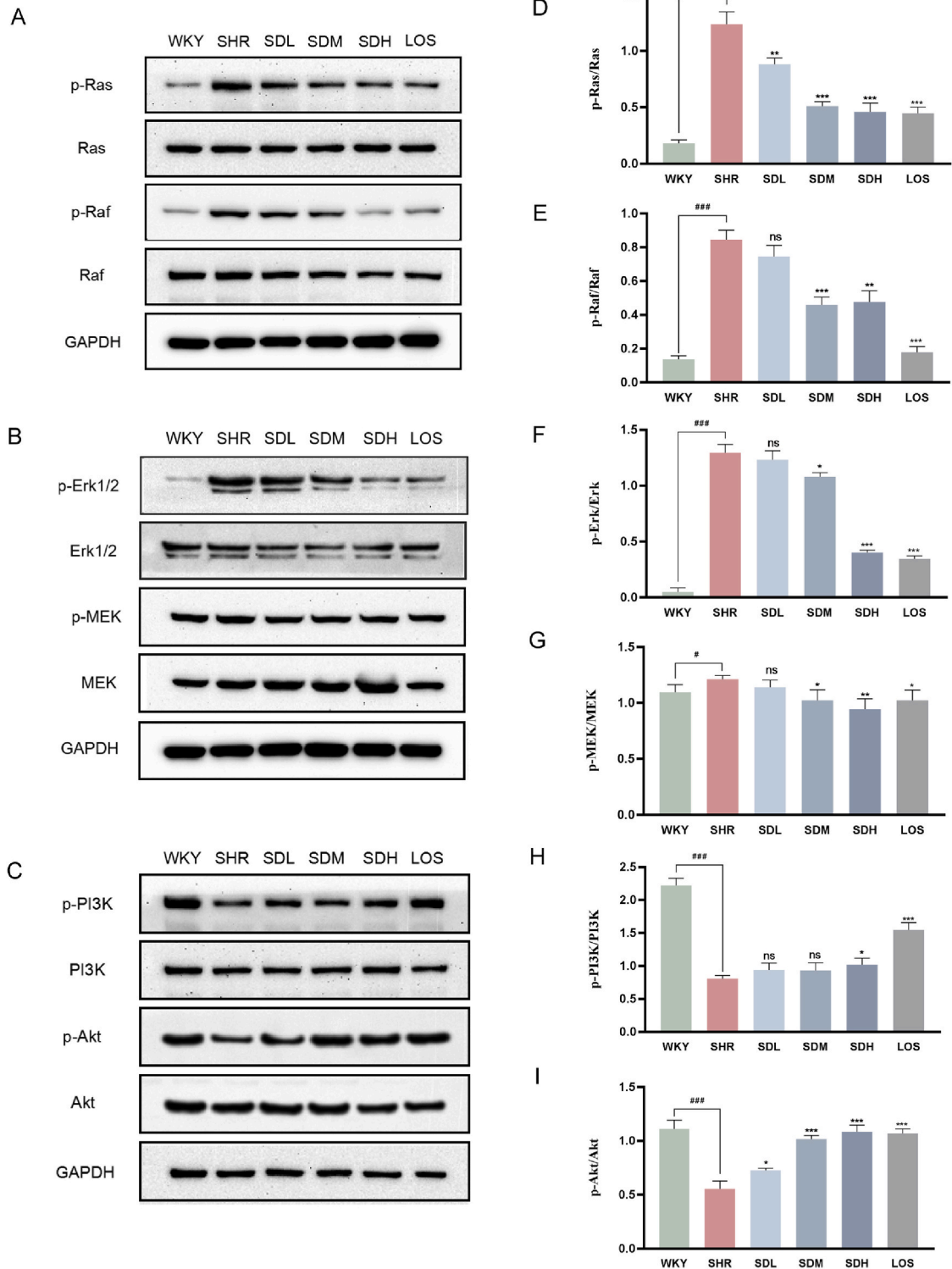


**Fig. 6.** Effect of Sal D on the Ras signalling pathway and PI3K/AKT signalling pathway in the myocardium. Protein expression of (A) p-Ras, Ras, p-Raf, Raf; (B) p-MEK, MEK, p-Erk, Erk; (C) p-PI3K, PI3K, p-Akt, Akt and (D–I) quantization in the myocardium. Results are presented as the mean  $\pm$  SEM (\* $P$  < 0.05, \*\* $P$  < 0.01 and \*\*\* $P$  < 0.001 vs. SHR; \* $P$  < 0.05, \*\* $P$  < 0.01 and \*\*\* $P$  < 0.001 vs. SHR; ### $P$  < 0.001 vs. WKY; ### $P$  < 0.001 vs. WKY).

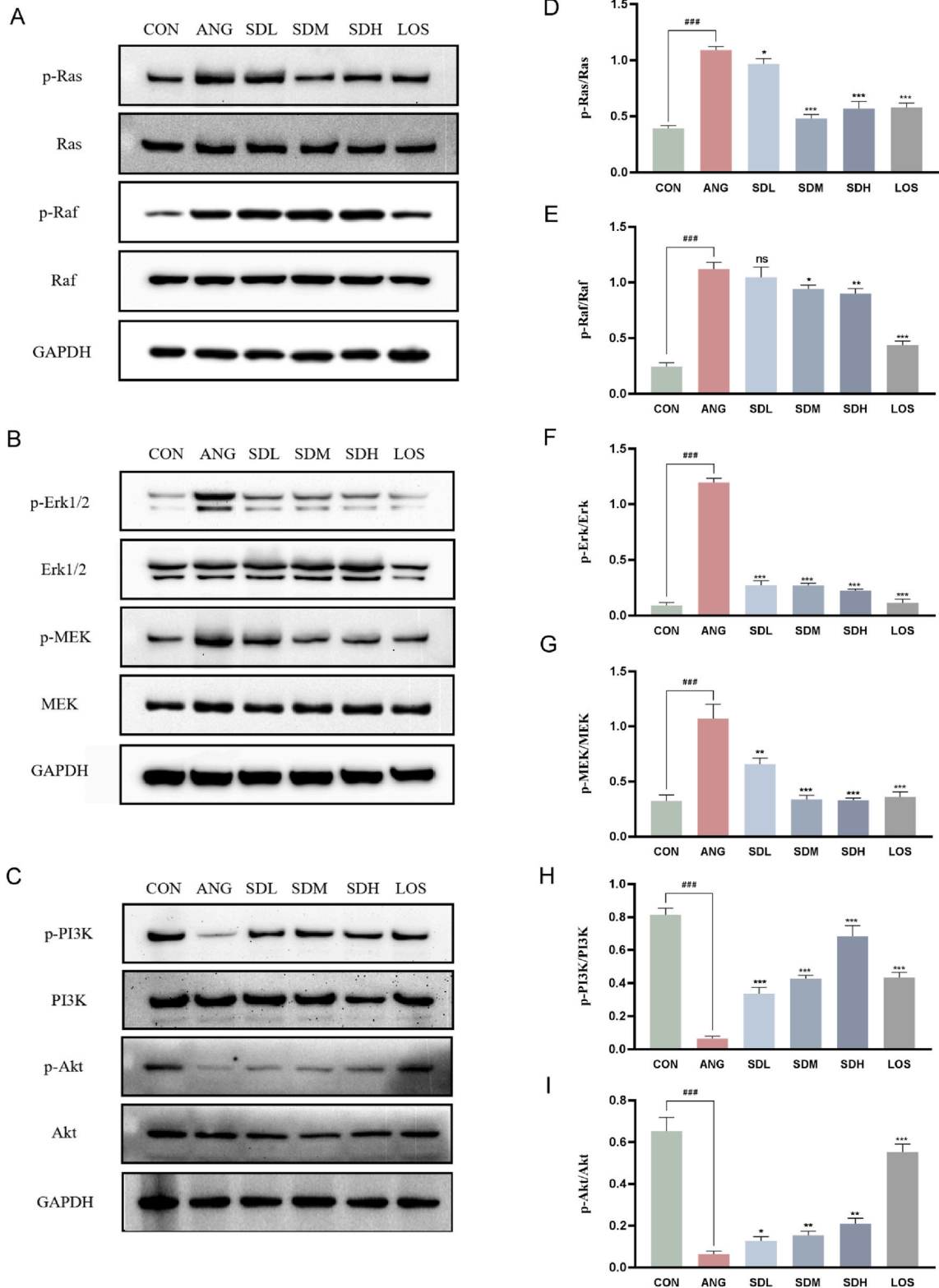
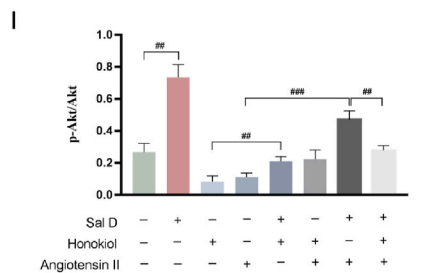
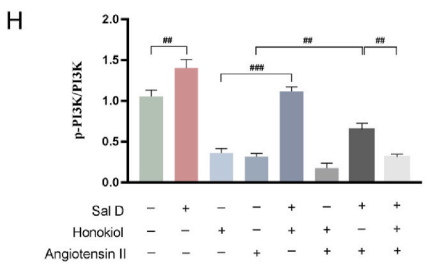
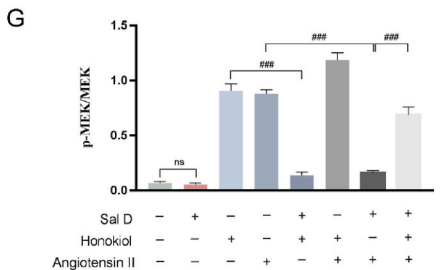
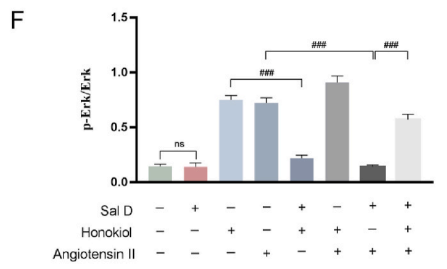
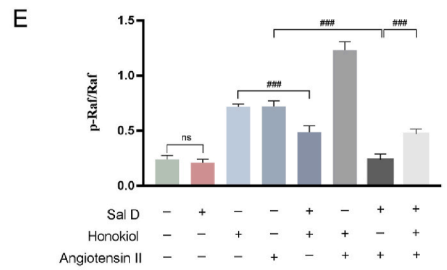
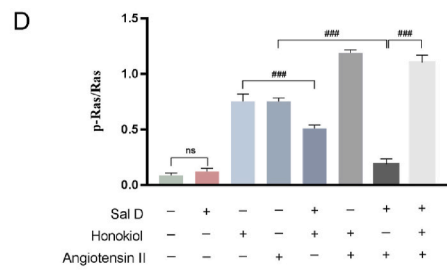
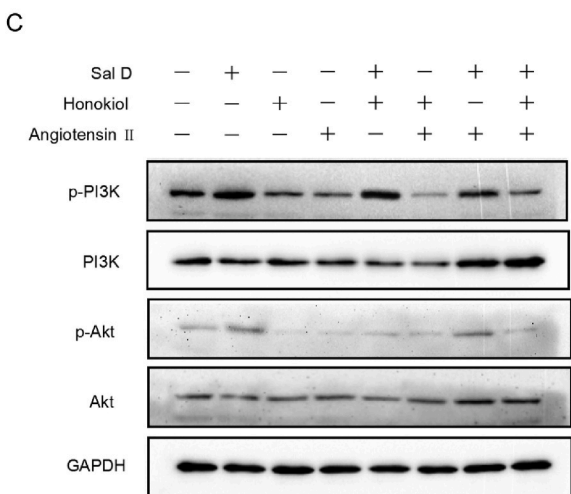
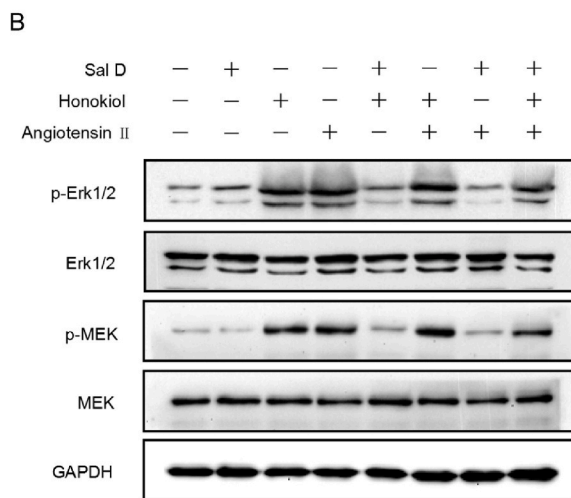
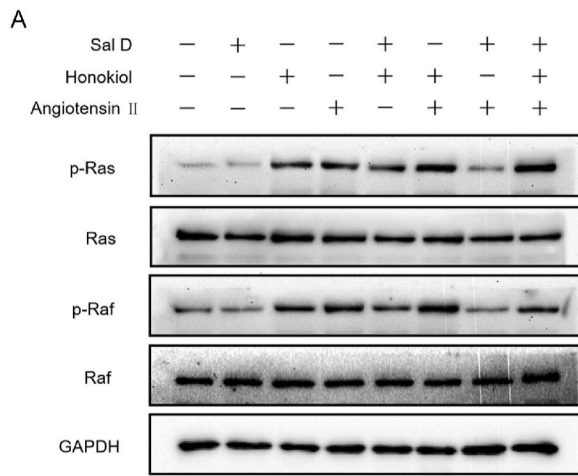


**Fig. 7.** Effect of Sal D on Ras signalling pathway and PI3K/AKT signalling pathway in cardiomyocytes. Protein expression of (A) p-Ras, Ras, p-Raf, Raf; (B) p-MEK, MEK, p-Erk, Erk; (C) p-PI3K, PI3K, p-Akt, Akt and (D–I) their quantization in **cardiomyocyte**. Results are presented as the mean  $\pm$  SEM (\* $P < 0.05$ , \*\* $P < 0.01$  and \*\*\* $P < 0.001$  vs. ANG; # $P < 0.05$ , ## $P < 0.01$  and ### $P < 0.001$  vs. CON).



(caption on next page)

**Fig. 8.** Effect of Sal D on Ras signalling pathway and PI3K/AKT signalling pathway in cardiomyocytes with Honokiol. Protein expression of (A) p-Ras, Ras, p-Raf, Raf; (B) p-MEK, MEK, p-Erk, Erk; (C) p-PI3K, PI3K, p-Akt, Akt and (D–I) their quantization in the myocardium. Results are presented as the mean  $\pm$  SEM. (<sup>#</sup> $P < 0.05$ , <sup>##</sup> $P < 0.01$ ).

analysis, the protein targets of Sal D were predicted. Prediction suggested that Sal D may improve HF through the following pathways: the Ras (Ras/Raf/MEK1/ERK) signalling pathway, the PI3K-AKT signalling pathway, the JAK-STAT signalling pathway, and HIF-1 signalling pathway, and so on. Since the Ras signalling pathway and the PI3K-AKT signalling pathway were highly enriched with a target level of 9, moreover, these two pathways are reported to be star signalling pathways associated with cardiac hypertrophy and cardiac dysfunction [18–20]. Thus, these two pathways were selected as the primary mechanism investigation of Sal D on HF.

Numerous signalling pathways have been characterized as being involved in heart remodelling. When cardiomyocytes work in bad conditions, they constantly endure neurohumoral attacks, such as angiotensin and endothelin-1, which via transmembrane receptors, activate downstream signalling pathways, trigger maladaptive cardiac hypertrophic response, and eventually contribute to HF. For instance, over-activation of the Ras/Raf/MEK1/ERK pathway can induce early response genes, loss of mitochondria function, and alteration in ion channel proteins in cardiomyocytes, all of which lead to pathological changes of the extracellular matrix, decreased cardiac output, and electrophysiological abnormalities [18]. And the PI3K/AKT signalling cascade, activated by growth factors, acts as a protecting role in compensatory hypertrophic response and systolic dysfunction, even guarding cardiomyocytes against apoptotic death [21,22]. Notably, AKT can effectively inhibit the activity of Raf by phosphorylating Raf. In HEK293 cells, activated AKT decreased the activity of Raf. The mechanism is that AKT phosphorylates Raf and provides a binding site of negative regulatory protein for Raf, thereby downregulating the activity of Raf. The inhibition of AKT by LY294002 can improve the activity of Raf [23].

In vivo and in vitro experimental data indicated that compared with the WKY group, the protein levels of p-Ras, p-Raf, p-Mek, and p-Erk were ascended, and the protein levels of p-PI3k and p-Akt were reduced in the SHR group. In contrast, after treatment with Sal D, the data mentioned above had been reversed. It illustrated that the mechanism of Sal D improving cardiac function is concerned with the suppression Ras signal pathway and activation of the PI3K/AKT signalling pathway. As an activator of the Ras signalling pathway and concurrently an inhibitor of PI3K/AKT signalling pathway, Honokiol was administrated to explore further if the active site of Sal D is indeed on the pathways, and also for the sake of excluding false-positive results. Compared with Sal D administrated alone, after being combined with Honokiol, cardiomyocyte data presented as the protein level of p-Ras, p-Raf, p-Mek, and p-Erk were significantly increased p-PI3k and p-Akt were decreased remarkably. The same phenomena occurred in phenotypic studies; with the management of Honokiol, the improvement of Sal D on mitochondrial dysfunction in cardiomyocytes was attenuated. That demonstrated that the anti-HF function of Sal D is achieved by regulating the Ras signalling pathway and PI3K/AKT signalling pathway. At the same time, Sal D no longer has a relevant effect when these pathways are blocked.

In summary, for the first time, our study proved Sal D is an effective active substance which can be applied to treat HF initiated by hypertension, manifested as reducing blood pressure, alleviating cardiac remodelling, and enhancing cardiac function, besides protecting the mitochondria through reducing ultrastructural damage of mitochondria, and attenuation of energy charge. The potential mechanism of Sal D in the treatment of HF is accomplished lies in inhibiting the Ras pathway and activating PI3K/AKT pathway simultaneously. There is some limitation in this study. For instance, protein p110/p85 was not detected, which exists in the crosstalk of these two pathways. Downstream signalling molecules of AKT were not further evaluated in this study, such as Bcl-2 and Bax, are essential proteins associated with apoptosis.

## Funding

This work was supported by the Natural Science Foundation of China (Project NO 82274292) and the Natural Science Foundation of Guangdong Province, China (Project NO 2021A1515011674, and G821291026).

## Author contribution statement

Lin LV and Guohua Zhang conceived and designed the experiments. Kai Chen performed the experiments and wrote the paper. Yiqing Guan analyzed and interpreted the data. Shaoyu Wu, Huanxian Wu and Dongling Quan Contributed reagents, materials, analysis tools or data. Lin LV and Guohua Zhang contributed equally to this work and should be considered correspondence authors. Each author has participated sufficiently in work to take public responsibility for appropriate portions of the content and agreed to be accountable for all aspects of the work in ensuring that questions related to the accuracy or integrity of any part of the work are appropriately investigated and resolved.

## Declaration of competing interest

The authors declared no potential conflict of interests concerning research, authorship, and publication of this paper.

## Acknowledgement

We would like to thank all the authors of this study for their exceptional cooperation and valuable contributions. Moreover, we thank the School of Pharmaceutical Science, Southern Medical University, Guangzhou, Guangdong Province, China, for providing

facilities for the present work.

## Appendix A. Supplementary data

Supplementary data related to this article can be found at <https://doi.org/10.1016/j.heliyon.2022.e12337>.

## References

- [1] B. Ziaiean, G.C. Fonarow, Epidemiology and aetiology of heart failure, *Nat. Rev. Cardiol.* 13 (6) (2016) 368–378, 2016-06-01.
- [2] J. Kuschyk, B. Rudic, V. Liebe, E. Tulumen, M. Borggrefe, I. Akin, [Cardiac contractility modulation for treatment of chronic heart failure], *Herzschrittmacherther Elektrophysiol.* 29 (4) (2018) 369–376, 2018-12-01.
- [3] Y. Tu, Artemisinin-A Gift from Traditional Chinese Medicine to the World (Nobel Lecture), *Angew. Chem. Int. Ed. Engl.* 55 (35) (2016) 10210–10226, 2016-08-22.
- [4] W. Chen, G. Chen, Danshen (*Salvia miltiorrhiza* Bunge): a prospective healing sage for cardiovascular diseases, *Curr. Pharmaceut. Des.* 23 (34) (2017) 5125–5135, 2017-01-20.
- [5] W. Zhang, J. Song, et al., Salvianolic acid D alleviates cerebral ischemia-reperfusion injury by suppressing the cytoplasmic translocation and release of HMGB1-triggered NF- $\kappa$ B activation to inhibit inflammatory response, *Mediat. Inflamm.* 2020 (2020) 9049614–9049615, 2020-01-01.
- [6] Z. Hu, H. Wang, et al., Danhong injection mobilizes endothelial progenitor cells to repair vascular endothelium injury via upregulating the expression of Akt, eNOS and MMP-9, *Phytomedicine* 61 (2019), 2019-01-01 152850-152850.
- [7] B. Jiang, D. Li, Y. Deng, F. Teng, J. Chen, S. Xue, et al., Salvianolic acid A, a novel matrix metalloproteinase-9 inhibitor, prevents cardiac remodeling in spontaneously hypertensive rats, *PLoS. One.* 8 (3) (2013), e59621, 2013-01-20.
- [8] Tanshinone I alleviates insulin resistance in type 2 diabetes mellitus rats through IRS-1 pathway, *Biomed. Pharmacother.* 93 (2017) 352–358, 2017-09-01.
- [9] X. Zhang, Q. Wang, et al., Tanshinone IIA protects against heart failure post-myocardial infarction via AMPKs/mTOR-dependent autophagy pathway, *Biomed. Pharmacother.* 112 (2019) 108599, 2019-04-01.
- [10] A.J. Wilson, V.Y. Wang, et al., Increased cardiac work provides a link between systemic hypertension and heart failure, *Phys. Rep.* 5 (1) (2017), 2017-01-01.
- [11] H.K. Gaggin, J.J. Januzzi, Biomarkers and diagnostics in heart failure, *Biochim. Biophys. Acta.* 1832 (12) (2013) 2442–2450, 2013-12-01.
- [12] J.L. Pohjoismäki, S. Goffart, The role of mitochondria in cardiac development and protection, *Free. Radic. Biol. Med.* 106 (2017 May) 345–354, <https://doi.org/10.1016/j.freeradbiomed.2017.02.032>. Epub 2017 Feb 17. PMID: 28216385.
- [13] A. Fukushima, K. Milner, et al., Myocardial energy substrate metabolism in heart failure : from pathways to therapeutic targets, *Curr. Pharmaceut. Des.* 21 (25) (2015) 3654–3664, 2015-01-20.
- [14] V. Lahera, N. de Las Heras, A. López-Farré, W. Manucha, L. Ferder, Role of Mitochondrial Dysfunction in Hypertension and Obesity, *Curr. Hypertens. Rep.* 19 (2) (2017 Feb) 11, <https://doi.org/10.1007/s11906-017-0710-9>. PMID: 28233236.
- [15] J. Ru, P. Li, J. Wang, W. Zhou, B. Li, C. Huang, et al., TCMSP: a database of systems pharmacology for drug discovery from herbal medicines, *J. Cheminform.* 6 (13) (2014), 2014-01-20.
- [16] Z. Liu, F. Guo, Y. Wang, C. Li, X. Zhang, H. Li, et al., BATMAN-TCM: a Bioinformatics analysis tool for molecular mechanism of traditional chinese medicine, *Sci. Rep.* 6 (2016), 21146, 2016-02-16.
- [17] X. Liu, S. Ouyang, B. Yu, Y. Liu, K. Huang, J. Gong, et al., PharmMapper server: a web server for potential drug target identification using pharmacophore mapping approach, *Nucleic. Acids. Res.* 38 (2010) W609–W614, 2010-07-01 (Web Server issue).
- [18] T. Yamazaki, I. Komuro, et al., Signalling pathways for cardiac hypertrophy, *Cell. Signal.* 10 (10) (1998) 693–698, 1998-11-01.
- [19] T. Shioi, P.M. Kang, P.S. Douglas, J. Hampe, C.M. Yballe, J. Lawitts, et al., The conserved phosphoinositide 3-kinase pathway determines heart size in mice, *Embo. J.* 19 (11) (2000) 2537–2548, 2000-06-01.
- [20] J. Luo, J.R. McMullen, C.L. Sobkiw, L. Zhang, A.L. Dorfman, M.C. Sherwood, et al., Class IA phosphoinositide 3-kinase regulates heart size and physiological cardiac hypertrophy, *Mol. Cell. Biol.* 25 (21) (2005) 9491–9502, 2005-11-01.
- [21] G.Y. Oudit, M.A. Crackower, U. Eriksson, R. Sarao, I. Kozieradzki, T. Sasaki, et al., Phosphoinositide 3-kinase gamma-deficient mice are protected from isoproterenol-induced heart failure, *Circulation* 108 (17) (2003) 2147–2152, 2003-10-28.
- [22] A. Rohini, N. Agrawal, C.N. Koyani, R. Singh, Molecular targets and regulators of cardiac hypertrophy, *Pharmacol. Res.* 61 (4) (2010) 269–280, 2010-04-01.
- [23] K.L. Guan, C. Figueroa, T.R. Brtva, et al., Negative regulation of the serine/threonine kinase B-Raf by Akt, *J. Biol. Chem.* 275 (35) (2000) 27354–27359.